INVESTIGATING THE STRUCTURAL TRANSFORMATION OF INDIVIDUAL Au-INCORPORATED CARBON NANOFIBER INTERCONNECT

Mohamad Saufi Rosmi[1,*], Yazid Yaakob[2], Mohd Zamri Mohd Yusop[3], Illyas Md Isa[1], Siti Munirah Sidik [1], Suriani Abu Bakar[4] and Tanemura Masaki[5]

[1]Department of Chemistry, Faculty of Science and Mathematics, Universiti Pendidikan Sultan Idris, 35900 Tanjong Malim, Perak, Malaysia
[2]Department of Physics, Faculty of Science, Universiti Putra Malaysia, 43400 UPM Serdang, Selangor, Malaysia
[3]Department of Materials, Faculty of Mechanical Engineering, Universiti Teknologi Malaysia, 81310 Skudai, Johor, Malaysia
[4]Department of Physics, Faculty of Science and Mathematics, Universiti Pendidikan Sultan Idris, 35900 Tanjong Malim, Perak, Malaysia
[5]Department of Physical Science and Engineering, Nagoya Institute of Technology, Gokiso-cho, Showaku, Nagoya 466-8555, Japan

[*]saufirosmi@fsmt.upsi.edu.my

Abstract. Nowadays, a smaller electronic integrated circuit demands a smaller width and pitch of interconnect. Copper (Cu) interconnect, which is currently the most common, suffers from the size effect and grain boundary scattering. Hence, carbon materials such as carbon nanotubes (CNTs) and carbon nanofiber (CNF), as well as their nanocomposites are potential replacement materials for Cu interconnects. However, the interaction of carbon atoms and its metal catalyst is quite critical for obtaining nanocarbon structure with precise layer number, crystal size and structure. Here, an in-situ transmission electron microscopy (TEM) observation of graphitic hollow structure growth from a single Au-incorporated carbon nanofiber (Au-CNF) during current-voltage (I-V) measurement is demonstrated. With an applied potential in a two-probe system, significant structural change of Au-CNF was discovered. Due to Joule heating and a considerable temperature gradient, the Au nanoparticles agglomerated and evaporated under high current flow ranging from 1.35 to 18.7 μA. The TEM images and electron diffraction pattern revealed that after the current flow, the amorphous carbon structure of CNF was converted to a hollow sp2 graphitic carbon structure catalyzed by dispersed Au particles. The graphitic carbon structure, however, collapsed in the center at a higher applied potential of 60 A due to excessive current flow and induced Joule heating. The direct observation of graphene synthesis thru in-situ TEM is important for revealing the solid phase interaction of Au and carbon atoms.

Keywords: Graphene, gold, solid phase reaction, in-situ TEM

Article Info

Received 19th December 2021
Accepted 26th November 2022
Published 23rd December 2022

ISSN: 1823-7010, eISSN: 2600-7444

Introduction

Carbon nanotubes (CNTs) and carbon nanofibers (CNFs) have attracted a lot of attention due to their attractive properties, which have led to a lot of research regarding their potential applications, including as VLSI interconnect materials. CNTs and CNF have become an alternative material to overcome the weaknesses of the current on-chip interconnect technology which uses copper (Cu)-based material [1-4]. Cu-based interconnects have a few weaknesses as copper resistivity increases fast when linewidth decreases, resulting in latency difficulties owing to both line resistance and load capacitance [5-7]. On top of that, Cu interconnect faces reliability issues due to electromigration [8,9].

Previous research employing carbon-based nanostructures for interconnects has shown promising initial electrical characterization data which inspire further research in this area. CNTs and CNF have been chosen as potential interconnect material due to their robust thermal, electrical and mechanical properties, in addition to their high-aspect ratio [10-14]. Previous studies have demonstrated the incorporation of metal such as Platinum (Pt) and Gold (Au) in CNF successfully improved the conductivity of the CNF as an interconnect [15,16]. This is due to the fact that the presence of metal increases contact morphology, which in turn improves resistance in the CNF structure.

While the contact resistance of CNF structures has been studied previously, the intrinsic properties of nanofibers, such as structural development during current flow have yet to be completely investigated for integrated circuit applications. The study on the behavior of the CNF interconnect structure is highly essential to maintain the stability of the structure. In recent studies of thermal and electrical transports in CNF, it is reported that the breakdown of CNF is more likely due to the Joule heating. Thus, this work was conducted to study the Au-incorporated CNF (Au-CNF) fundamental structural evolution during high current flow at high bias voltage (up to 1.5 V) using in-situ transmission electron microscopy (TEM).

Materials and Methods

Figure 1(a) demonstrates the schematic illustration for fabrication of Au-CNF. For the Au-CNF fabrication, a commercially available graphite foil (5 mm x 25 mm x 100 μm in thickness) and Kaufmann-type ion gun with 6 cm ion beam diameter and 1 keV energy (Iontech. Inc. Ltd., model 3-1500-100FC) were used in this study. Graphite foil was mounted to the sample stage and an Au plate, which served as the Au atom supply, was positioned at the graphite foil's edge. Ion irradiation was performed onto the edges of graphite foil and Au plate for 60 minutes at ion incident angle of 45^{o} from normal to the graphite and Au surface. For the fabrication of Au-CNF, the basal and working pressures exerted were 1.5 x 10^{-5} and 2.0 x 10^{-2} Pa, respectively. The morphology of the graphite surface was characterized using scanning electron microscope (SEM) (Jeol JEM- 5600). As seen in Figure 1(b), the structure consists of conical protrusions with one Au-CNF growing on the tip. CNFs grew as a result of ion irradiation because of the redeposition of sputter-ejected carbon atoms onto the sidewalls of the conical protrusions and the excess surface diffusion of carbon atoms to the tips during Ar sputtering (Figure 1(c)).

A TEM sample holder (JEOL; EM-Z02154T) with a tungsten nanoprobe as an anode was employed for in-situ current – voltage (I-V) TEM measurements (Figure 1(d)). The Au-CNF was placed on the stationary stage of TEM and functioned as a cathode. This TEM

holder comprises of electrical biasing equipment which allows the monitoring of the morphological change of Au-CNF during current flow. The structural transformation of Au-CNF was carefully observed with TEM (JEOL JEM 2010) while controlling the bias voltage throughout the process. A vacuum chamber in TEM was operated at a pressure of less than 2.5 x 10^{-5} Pa and a 200 kV acceleration voltage. Image recording software was used to capture TEM pictures in video mode.

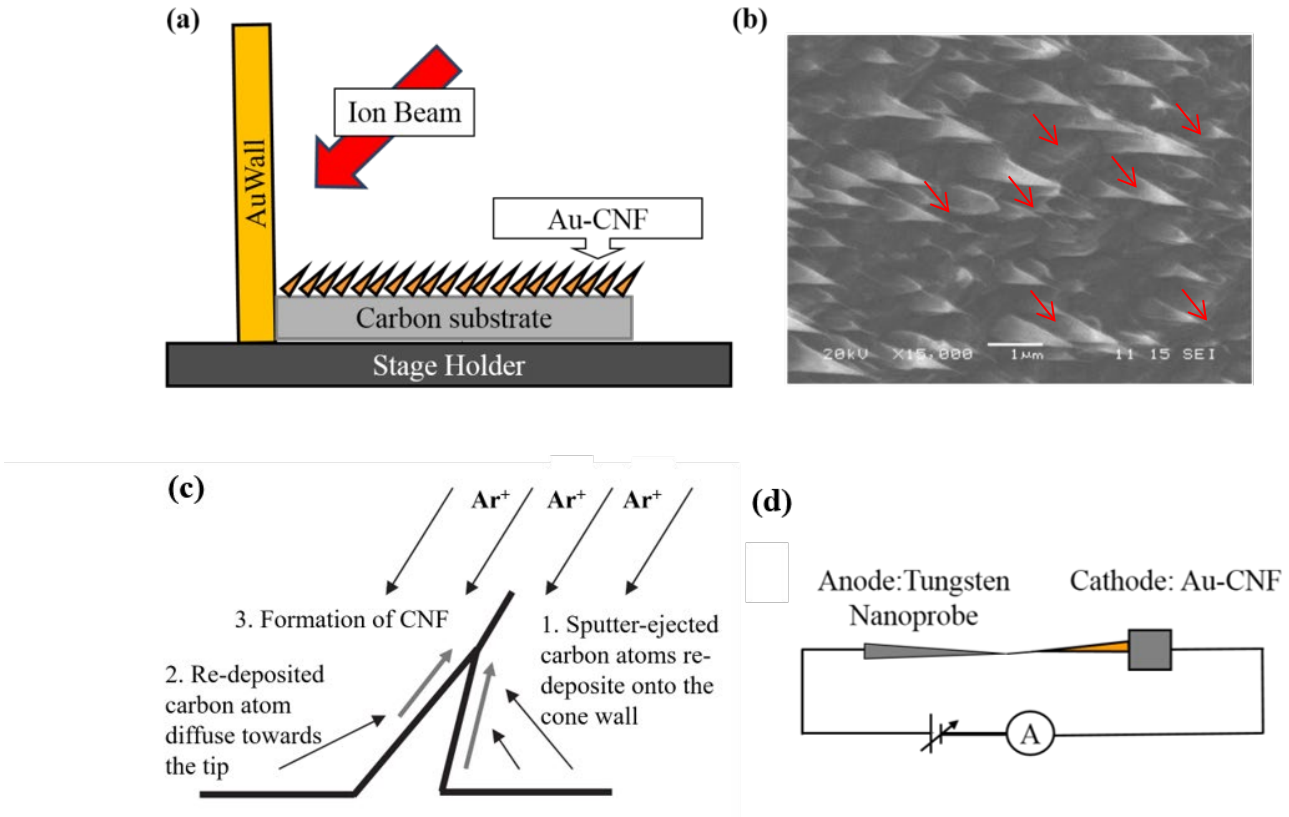

Figure 1: (a) The experimental setup for the fabrication of Au-CNF is depicted schematically, (b) Au-CNF SEM image at the graphite foil edge, (c) Schematic representation of CNF growth mechanism and (d) Schematic representation of the experimental setup for in-situ TEM I-V measurement.

Results and Discussion

The characterization of a single Au-CNF is shown in Figure 2(a) to (c). The length and diameter of Au-CNF in Figure 2(a) were 500 nm and 10 nm, respectively. Figure 2(b) depicts the TEM image of the cone (base), and Figure 2(c) represents the middle area of the Au-CNF. It can be seen that the Au nanoparticles with diameters ranging from 5 to 15 nm were uniformly dispersed throughout the carbon matrix. Figure 2(d) depicts the CNF's selected area electron diffraction (SAED) pattern in the region labelled "A" in Figure 2(a). From the pattern, it can be seen that Au-CNF consist of a combination of randomly oriented Au nanoparticle and amorphous carbon.

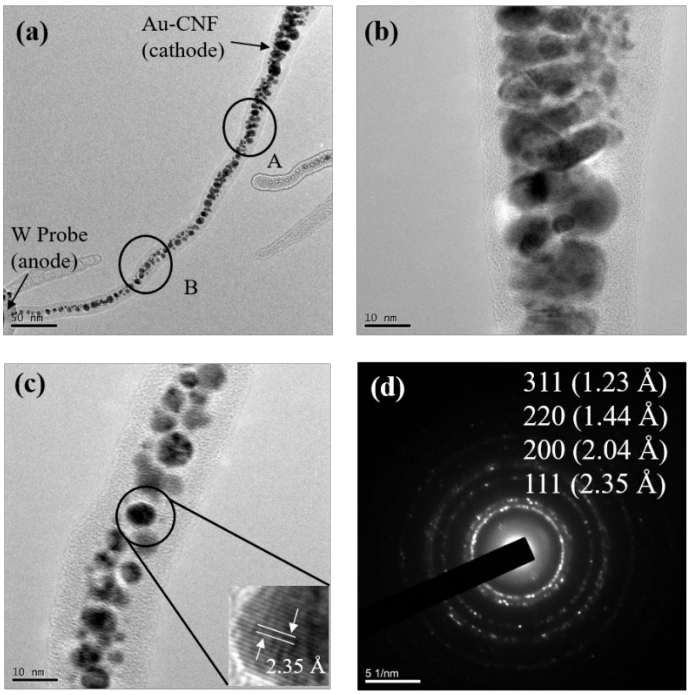

Figure 2: (a) TEM image of the Au-CNF prior to I-V measurement, high magnification TEM image of the Au-CNF in (b) region A and (c) region B, the inset of (c) display the high magnification image of the Au nanoparticle and (d) SAED pattern of the Au-CNF taken at a region abbreviated as A.

Figure 3(a) displays the I-V characteristics of Au-CNF where it can be seen that up to 0.56 V applied voltage, there is only a small amount of current flow presence (maximum current flow: 10^{-6} A). This is believed to be due to the high resistance in the amorphous structure of CNF. In amorphous carbon, the electrical transport is contributed from the hopping mechanism where the transmission of electron occurs over the orbital of different species. The tunnelling transition between localised states occurs here, where the difference in energy between the initial and final states is likely due to electron-phonon scattering [17]. As the applied voltage increased up to 0.56 V, the calculated resistance is 0.3 MΩ, which is almost similar to the value described for an amorphous carbon [18]. At applied voltage of 0.57 V, there is significant increase in the current flow where the resistance suddenly drops from 0.3 MΩ to 50 kΩ. Figure 3(b) and (c) show TEM images of Au-CNF after an applied voltage of 1V. It can be seen that Au nanoparticles have agglomerated and poor crystalline structure had started to form around the surface of Au as an effect of resistive Joule heating. Joule heating is the physical effect of a current passing through an electrical conductor producing thermal energy. A TEM image of a low crystalline graphitic structure is shown in Figure 3(c). During the current flow, Au nanoparticle starts to agglomerate and affect the amorphous carbon around it to recrystallize to form sp2 carbon structure. To understand more about the graphitic layer formation around Au nanoparticle, the experiment was further conducted at higher applied potential.

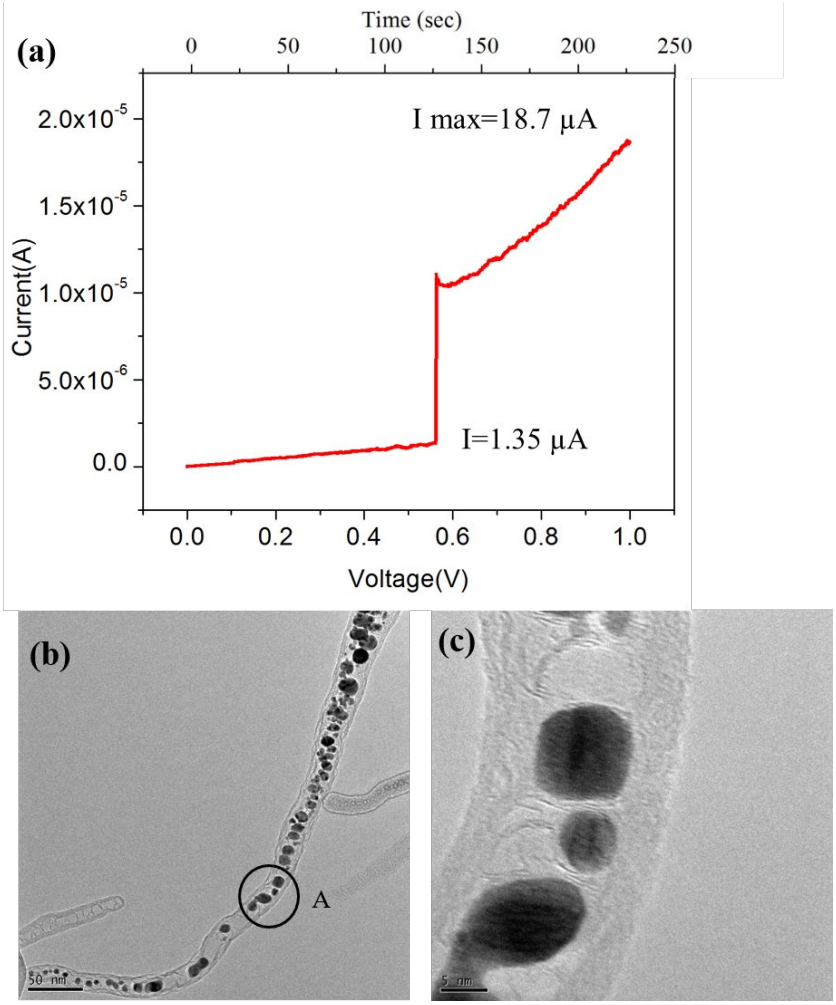

Figure 3: (a) I-V characteristic of the Au-CNF at lower applied voltage, (b) TEM image of Au-CNF after lower applied potential and (c) The high magnification image of Au-CNF after lower applied potential at region A.

Figure 4(a) shows the Au-CNF's I-V curve at a higher applied voltage. The current flow continues to increase until it reaches 20 A (at 1.0 V) with a resistance of 55 kΩ. As a voltage of more than 1.0 V was applied, the current flow increased significantly, while the resistance dropped from 55 kΩ to 14 kΩ. When a high current flowed through the low diameter CNF, major structural change of the Au-CNF happened due to Joule heating. After 201 seconds of current flow, the Au nanoparticles at the core of the Au-CNF began to evaporate (more than 1.30 V) as shown in Figure 4(b). This may be due to the very high temperature at the middle part of CNF resulting from Joule heating, whereby the tip of CNF will act as a heat sink [19]. The Au nanoparticle continued to evaporate till it reached applied bias of 1.5 V, leaving a hollow graphitic carbon structure. It is important to mention that only hollow graphitic carbon structure was left when Au particles evaporated. Finally, the in-situ TEM effectively synthesized a hollow graphitic carbon structure with a length of roughly 500 nm and width between 10 and 15 nm. In our earlier report about the field emission process of iron (Fe) - included CNF, Joule heating occurred, resulting in the agglomeration and electromigration of Fe nanoparticle causing the formation of carbon nanotubes (CNT) [20]. This contradicts with the result from the Au-CNF where the Au neither agglomerates nor migrates after the Joule heating effect. This is because Au possesses lower evaporation temperature compared to Fe nanoparticle, which leads to faster evaporation phenomenon

caused by heat generated from the Joule heating phenomenon. In comparison to bulk carbon atom diffusion, the graphitization process in Au-CNF could be considered as surface adsorption or diffusion [21]. The graphitization here is referring to the process of heating amorphous carbon for an extended period of time in order to reorganize the atomic structure and achieve the ordered crystalline structure typical of solids. Carbon atoms are rearranged during graphitization to fill atom vacancies and improve atom layout.

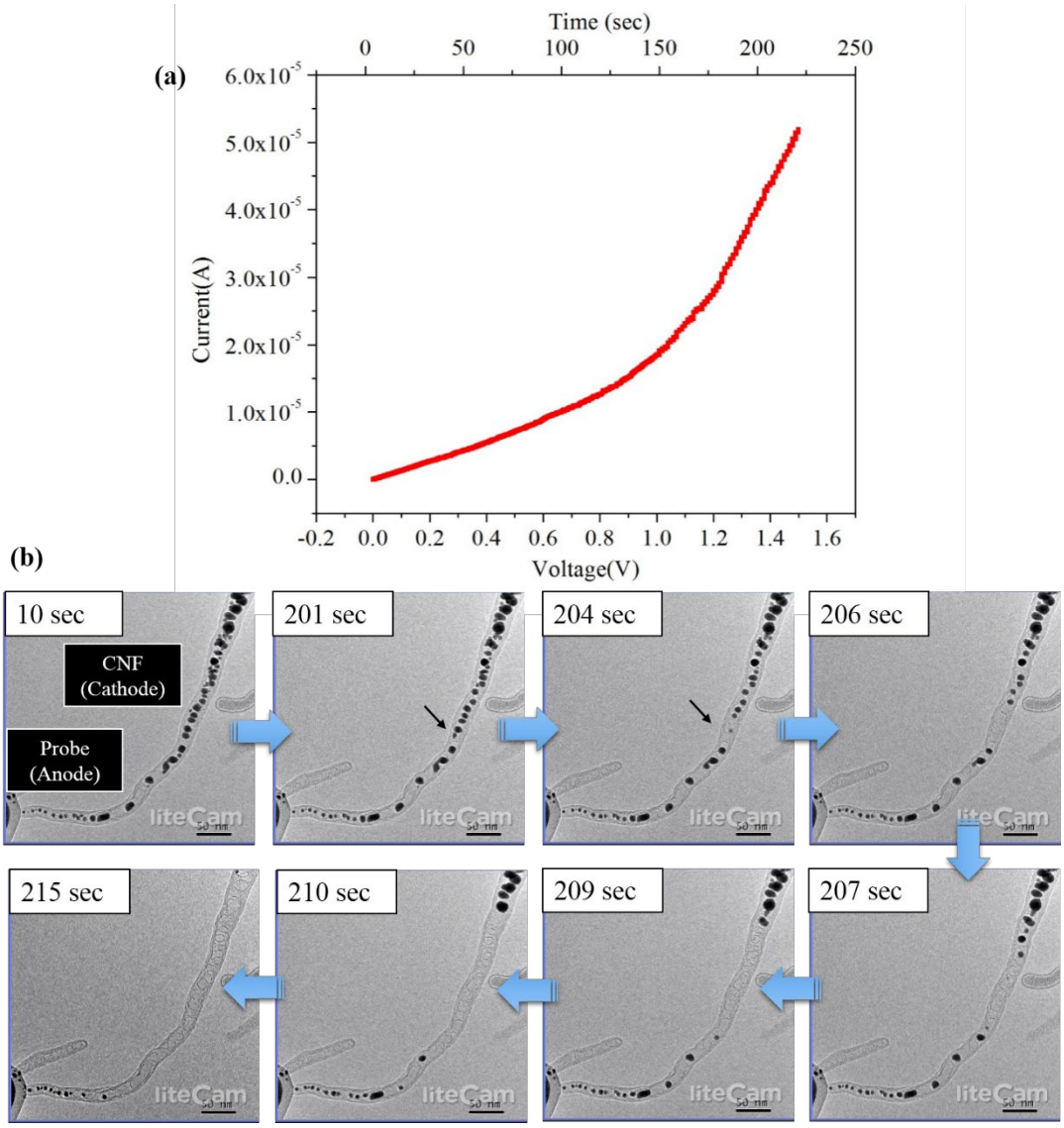

Figure 4: (a) I-V characteristic of the Au-CNF during the application of a higher bias voltage (0–1.5 V) and (b) *In-situ* TEM images of Au-CNF with applied potential changed from 0.0 to 1.5 V, as in the I-V characteristics.

Figure 5(a) shows a TEM image of the hollow graphitic carbon structure after the Au nanoparticles have been completely evaporated. As illustrated in Figure 5(a), the Au particles disappeared from the Au-CNF structure, leaving only the hollow graphitic carbon structure. Figure 3(a) showed an inset of the SAED analysis graphitic carbon structure, which revealed a ring pattern of polycrystalline structures. The absence of Au particles and the graphitization of Au-CNF to graphene-like hollow structure is confirmed by this SAED data. Higher

magnification TEM images were collected to prove this. Figure 5(b) shows a TEM image of a graphene-like hollow graphitic structure at high magnification. The synthesis of the sp2 hollow graphitic carbon structure is catalyzed by Au nanoparticles. The inter-planer spacing is approximately 0.345 nm, which corresponds to the graphite (0002) spacing. Surprisingly, the size of distributed Au particles corresponded to the area where the hollow graphitic structure appeared.

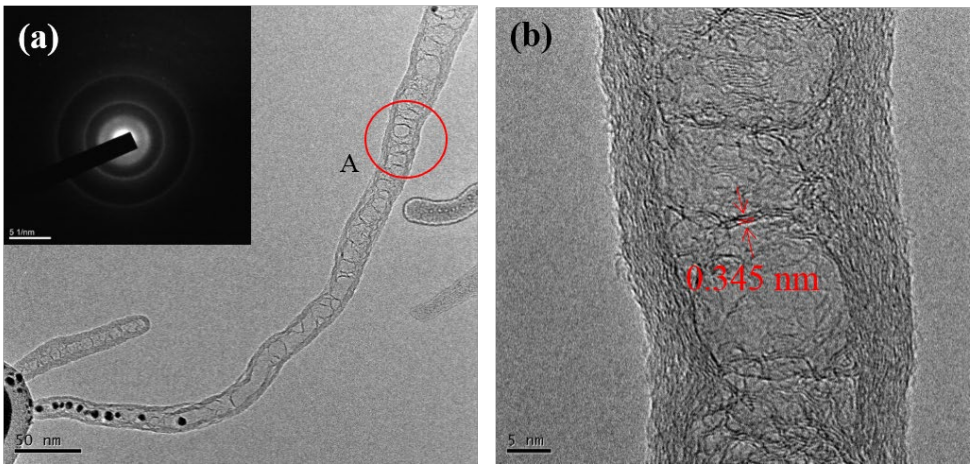

Figure 5: TEM image of the (a) hollow graphitic carbon structure after complete growth process and (b) hollow graphitic carbon structure in high magnification.

Figure 6(a) displays the I-V characteristics when maximum voltage was applied throughout the Au-CNF structure. It can be clearly observed that the current flow increases gradually while the remaining Au near the tip of CNF evaporated. However, during the process the hollow graphitic structure broke at the middle part of the structure due to saturated current flow at low area and production of high Joule heat. At 2.0 V applied voltage, a maximum current flow of 70 µA was obtained before a sharp decrease occurred due to the breaking of the structure. This demonstrates that a significant amount of heat is created among the metal contact in Au-CNF, reducing the structural strength of the hollow graphitic structure.

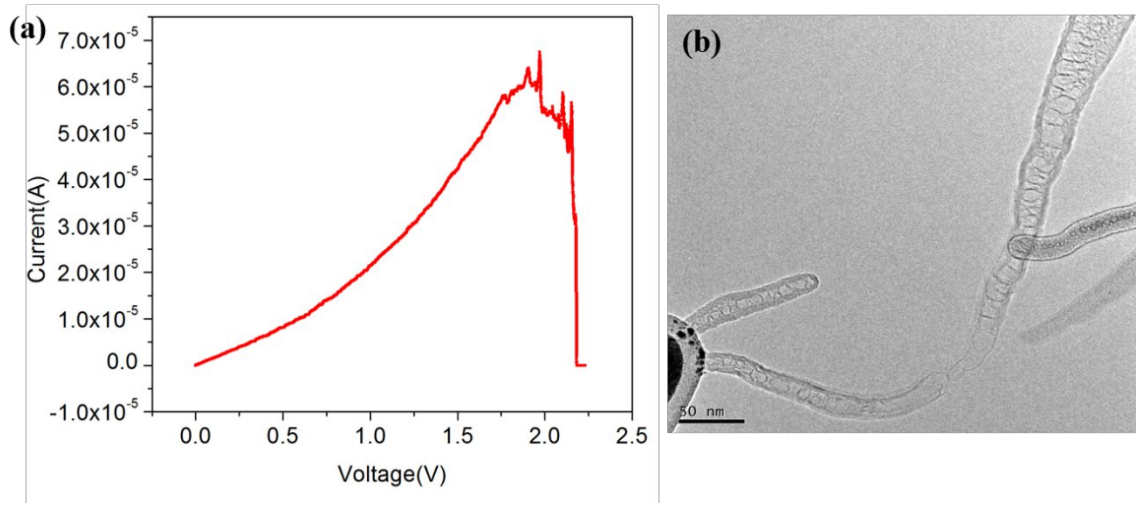

Figure 6: (a) I-V characteristic with maximum applied voltage across Au-CNF and (b) TEM image of the broken hollow graphitic carbon structure (~500 nm)

Conclusions

In a nutshell, the solid phase reaction between Au and carbon atoms as a potential candidate for interconnects when the current flow ranged from 1.35 to 20 μA was revealed. The construction of hollow graphitic structure was promoted by scattered Au nanoparticles inside the Au-CNF structure during the evaporation of the Au nanoparticles. A hollow graphitic carbon structure with a length of approximately 500 nm across the cathode and anode of an in-situ TEM was successfully observed. The reported hollow graphitic carbon structure development in nanoscale thru the in-situ TEM technique is important in understanding the interaction of carbon atoms with Au.

Acknowledgements

This study was supported by university research grant (GPU) through Universiti Pendidikan Sultan Idris, Malaysia (GPU-2017-0145-101-01). Also, the author would like to thank Nagoya Institute of Technology, Japan for the TEM facility.

Authors Contributions

All authors contributed toward data analysis, drafting and critically revising the paper and agree to be accountable for all aspects of the work.

Disclosure of Conflict of Interest

The authors have no disclosures to declare.

Compliance with Ethical Standards

The work is compliant with ethical standards.

References

[1] Ladani, L., Awad, I., She, Y., Dardona, S. & Schmidt, W. (2017). Fabrication of carbon nanotube/copper and carbon nanofiber/copper composites for microelectronics. *Materials Today Communications*, 11, 123-131.

[2] Mirza Gheitaghy, A., Poelma, R. H., Sacco, L., Vollebregt, S. & Zhang, G. Q. (2020). Vertically-aligned multi-walled carbon nano tube pillars with various diameters under compression: pristine and NbTiN coated. *Nanomaterials*, 10(6), 1189.

[3] Todri-Sanial, A., Ramos, R., Okuno, H., Dijon, J., Dhavamani, A., Widlicenus, M., Katharina L. & Teo, K. (2017). A survey of carbon nanotube interconnects for energy efficient integrated circuits. *IEEE Circuits and Systems Magazine*, 17(2), 47-62.

[4] Kim, I. T., Shin, S. & Shin, M. W. (2018). Development of 3D interconnected carbon materials derived from Zn-MOF-74@ carbon nanofiber web as an efficient metal-free electrocatalyst for oxygen reduction. *Carbon,* 135, 35-43.

[5] Weng, C. J. (2010). Nanotechnology copper interconnect processes integrations for high aspect ratio without middle etching stop layer. *Materials Science in Semiconductor Processing*, 13(1), 56-63.

[6] Pyzyna, A., Bruce, R., Lofaro, M., Tsai, H., Witt, C., Gignac, L., Brink, M. & Park, D. G. (2015). Resistivity of copper interconnects beyond the 7 nm node. In Proceedings of 2015 Symposium on VLSI Technology (VLSI Technology), 2015 Symposium on VLSI Technology (VLSI Technology), Japan, 16-18 June 2015.

[7] Roy, A. (2014). Fabrication and characterization of copper interconnects of line-width down to 100 nm using a specially designed phase shift mask. *Microelectronic Engineering*, 113, 152-156.

[8] Kato, T., Suzuki, K. & Miura, H. (2017). Effect of the crystallinity on the electromigration resistance of electroplated copper thin-film interconnections. *Journal of Electronic Packaging*, *139*(2), 020911.

[9] Sun, Z., Demircan, E., Shroff, M. D., Cook, C. & Tan, S. X. D. (2018). Fast electromigration immortality analysis for multisegment copper interconnect wires. *IEEE Transactions on Computer-Aided Design of Integrated Circuits and Systems*, 37(12), 3137-3150.

[10] Saito, T., Yamada, T., Fabris, D., Kitsuki, H., Wilhite, P., Suzuki, M. & Yang, C. Y. (2008). Improved contact for thermal and electrical transport in carbon nanofiber interconnects. *Applied Physics Letters*, 93(10), 102108.

[11] Kitsuki, H., Yamada, T., Fabris, D., Jameson, J. R., Wilhite, P., Suzuki, M. & Yang, C. Y. (2008). Length dependence of current-induced breakdown in carbon nanofiber interconnects. *Applied Physics Letters*, 92(17), 173110.

[12] Ladani, L., Awad, I., She, Y., Dardona, S. & Schmidt, W. (2017). Fabrication of carbon nanotube/copper and carbon nanofiber/copper composites for microelectronics. *Materials Today Communications*, 11, 123-131.

[13] Wilhite, P., Uh, H. S., Kanzaki, N., Wang, P., Vyas, A., Maeda, S., Yamada T. & Yang, C. Y. (2014). Electron-beam and ion-beam-induced deposited tungsten contacts for carbon nanofiber interconnects. *Nanotechnology*, 25(37), 375702.

[14] Wilhite, P., Vyas, A. A., Tan, J., Tan, J., Yamada, T., Wang, P., Park J. & Yang, C. Y. (2014). Metal–nanocarbon contacts. *Semiconductor Science and Technology*, 29(5), 054006.

[15] Vyas, A. A., Madriz, F., Kanzaki, N., Wilhite, P., Sun, X., Yamada, T. & Yang, C. Y. (2014). Carbon nanofiber interconnect RF characteristics improvement with deposited tungsten contacts. *Journal of Nanoscience and Nanotechnology*, 14(3), 2683-2686.

[16] Ueno, K., Takagi, M., Yano, H., Wakui, T., Yamazaki, Y., Sakuma, N., Kajita, A. & Sakai, T. (2013). Low-resistance metal contacts for nanocarbon/cobalt interconnects. *Japanese Journal of Applied Physics*, 52(5S3), 05FD01.

[17] Umeyama, T. & Imahori, H. (2018). Electron transfer and exciplex chemistry of functionalized nanocarbons: effects of electronic coupling and donor dimerization. *Nanoscale Horizons*, 3(4), 352-366.

[18] Rosmi, M. S., Yusop, M. Z., Kalita, G., Yaakob, Y., Takahashi, C. & Tanemura, M. (2014). Visualizing copper assisted graphene growth in nanoscale. *Scientific Reports*, 4(1), 1-6.

[19] Li, X., Zhao, L., Li, P., Zhang, Q. & Wang, M. S. (2017). In-situ electron microscopy observation of electrochemical sodium plating and stripping dynamics on carbon nanofiber current collectors. *Nano Energy,* 42, 122-128.

[20] Zamri Yusop, M., Kalita, G., Yaakob, Y., Takahashi, C. & Tanemura, M. (2014). Field emission properties of chemical vapor deposited individual graphene. *Applied Physics Letters*, 104(9), 093501.

[21] Takahashi, C., Yaakob, Y., Yusop, M. Z. M., Kalita, G. & Tanemura, M. (2014). Direct observation of structural change in Au-incorporated carbon nanofibers during field emission process. *Carbon*, 75, 277-280.